Anna Korzeń (korzen@mech.pk.edu.pl)

Institute of Thermal Power Engineering, Faculty of Mechanical Engineering, Cracow University of Technology

Dawid Taler

Institute of Heat Engineering and Air Protection, Faculty of Environmental Engineering, Cracow University of Technology

Mathematical modelling of the unsteady operation of a plate and fin heat exchanger for the time-varying mass flow rate of liquid and air velocity

Modelowanie matematyczne pracy wymiennika ciepła z rur ożebrowanych dla zmiennych w czasie strumienia masy płynu i prędkości powietrza

Abstract

The mathematical simulation of a plate fin and tube heat exchanger is presented in this paper. The simulation of the transient operation of the heat exchanger was carried out using a general numerical model that was previously developed by the authors. The Reynolds number of the water flowing inside the tubes varied in the range from 4000 to 12000. A detailed analysis of the transient response of a heat exchanger to sudden increase in water mass flow rate and the simultaneous reduction in air flow velocity was modelled. Heat transfer correlations for air and water were determined based on the experimental data. Unknown parameters appearing in the relationships for the Nusselt numbers on the air- and water-sides were estimated using the least squares method. A set of partial differential equations for the temperature of water, air, tube wall, and fins was solved using the finite volume method. The results of the numerical simulations of a heat exchanger using experimentally determined air and water-side heat transfer formulas for the calculation of heat transfer coefficients were compared with the experimental data. Excellent agreement between computation results (air and water temperatures at the outlet of the heat exchanger) and experimental results was obtained.

Keywords: plate-fin and tube heat exchanger; experimental determination of heat transfer correlations; numerical modelling; transient response; transition tube flow

Streszczenie

Przedstawiona została symulacja matematyczna wymiennika ciepła z rur ożebrowanych. Symulacja nieustalonej pracy wymiennika przeprowadzona została za pomocą modelu matematycznego opracowanego wcześniej przez autorów. Liczba Reynoldsa po stronie wody zmieniała się w zakresie od 4000 do 12 000. Szczegółowa analiza zmian temperatury została przeprowadzona dla przypadku nagłego wzrostu strumienia masowego płynu z jednoczesnym obniżeniem prędkości powietrza. Korelacje na współczynniki wnikania ciepła dla powietrza i wody określono na podstawie danych doświadczalnych. Nieznane parametry, które pojawiają się w równaniach na liczbę Nusselta dla powietrza i wody wyznaczono za pomocą metody najmniejszych kwadratów. Układ równań różniczkowych cząstkowych umożliwiający wyznaczenie temperatury wody, powietrza, ścianki rury i żeber zostały rozwiązane z użyciem metody objętości skończonej. Wyniki numerycznej symulacji pracy wymiennika z użyciem współczynników wnikania ciepła wyznaczonych z korelacji na liczby Nusselta od strony powietrza i wody porównano z danymi eksperymentalnymi. Uzyskano bardzo dobrą zgodność wyników obliczeń i pomiarów.

Słowa kluczowe: instalacje energetyczne, badania termowizyjne, termogram, emisyjność, temperatura odbicia

Nomenclature

A	–	surface area, m^2
A_{oval}	–	area of the oval opening in the fin, m^2
a, b	–	minor and major semi-axis of the inner tube surface, m
c_p	–	specific heat at constant pressure, J/(kg·K)
c_1, c_2, c_3	–	constants
d_h	–	air-side hydraulic diameter, m
d_r	–	water-side hydraulic diameter of the tube, m
f_1, f_2	–	mean air temperature at the inlet and outlet of the heat exchanger, °C or K
h	–	heat transfer coefficient, W/(m^2·K)
h_o	–	weighted heat transfer coefficient of the fin at the surface, W/(m^2·K)
k	–	thermal conductivity, W/(m·K)
L_{ch}	–	tube length in the radiator, m
m	–	mass, kg
$\dot{m}$	–	mass flow rate, kg/s
n_r	–	number of tubes
N	–	number of heat transfer units
Nu_1	–	liquid-side Nusselt number, $Nu_1 = h_1/d_r/k_1$
Nu_2	–	air-side Nusselt number, $Nu_2 = h_2/d_h/k_2$
p_1, p_2	–	transversal and longitudinal tube pitch, m
Re_1	–	liquid-side Reynolds number, $Re_1 = w_1\rho_1 d_r/\mu_1$
Re_2	–	air-side Reynolds number, $Re_2 = w_2\rho_2 d_h/\mu_2$
s	–	fin pitch, m
t	–	time, s
T	–	temperature, °C or K
U	–	tube perimeter, m
w	–	velocity, m/s
x, y	–	Cartesian coordinates, m
x^+	–	non-dimensional coordinate, $x^+ = x/L_{ch}$
y^+	–	non-dimensional coordinate, $y^+ = y/p_2$

Greek symbols

δ	–	thickness, m
Δx	–	control volume length, m
η	–	fin efficiency
μ	–	dynamic viscosity, kg /(m s)
ρ	–	density, kg/m^3
τ	–	the time constant, s

Subscripts

1 – fluid (water) flowing in the tube
2 – fluid *I don't think that air can be described as a fluid* (air) flowing perpendicularly to the tube axis
bbf – surface of a bare tube between fins
bo – outer surface of a bare tube
f – fin
in – inner surface of a tube
l – laminar
m – mean
T – uniform tube wall temperature
w – tube wall

1. Introduction

Publications on the dynamics of plate fin and tube heat exchangers (PFTHE) are limited in number. Mathematical models of heat exchangers that simulate non-steady state operation are needed to analyze the start-up and shutdown of heat exchangers. Dynamical models of heat exchangers are also used in PID control systems as well as in model-based control systems. However, a steady state of heat exchangers is analyzed in most of the works [1].

The transient response of the PFTHE was modelled in [2–6]. Usually, fins are modelled as elements with lumped thermal capacity while the equivalent heat transfer coefficient on the air side is calculated assuming the steady-state [2–6]. The steady-state temperature distribution in fins is used to determine the equivalent heat transfer – this simplification can lead to some errors, especially for higher fins.

The system of governing differential equations is solved by the Laplace transform or the finite difference method. The Laplace transform method has been widely used by Roetzel and Xuan [2] to model the transient operation of various heat exchangers. Taler [4] modelled the transient response of the PFTHE for a stepwise increase in liquid or gas temperature using the Laplace transform method. The transient temperature of the fluids was compared with temperature obtained by the finite volume method.

Korzeń and Taler [6] developed a new mathematical model of the PFTHE to simulate its transient operation. In contrast to the existing methods for the modelling of the transient response of heat exchangers with extended surfaces in which the weighted steady-state heat transfer coefficient on the finned tube side is used, the transient temperature distribution is calculated in each fin. This allows for a more exact computation of the heat flow rate from the fins to the flowing gas.

Usually, modelling PFTHEs assumes that the fluid flow inside the tubes is turbulent. However, many low-duty heat exchangers operate in the transitional region when the Reynolds number varies in the range of 2,300 to around 12,000.

In this paper, the numerical modelling of the transient work of a PFTHE for a low Reynolds numbers on the liquid side is carried out.

2. Mathematical formulation of the problem

The system of partial differential equations describing the space and time changes of liquid T_1, tube wall T_w, and air T_2 temperatures in one-row plate-fin and tube heat exchangers are [6]:

▸ liquid

$$\frac{1}{N_1}\frac{\partial T_1}{\partial x^+}+\tau_1\frac{\partial T_1}{\partial t}=-\left(T_1-T_w\right) \tag{1}$$

▸ tube wall

$$U_m\delta_w\rho_w c_w\frac{\partial T_w}{\partial t}+\frac{m_f c_f}{s}\frac{\partial \overline{T}_f}{\partial t}=\frac{k_w U_m\delta_w}{L_{ch}^2}\frac{\partial^2 T_w}{\partial\left(x^+\right)^2}+h_w U_{in}\left(T_1-T_w\right)+h_o U_{bo}\left(\overline{T}_2-T_w\right) \tag{2}$$

▸ air

$$\frac{1}{N_2}\frac{\partial T_2}{\partial y^+}+\tau_2\frac{\partial T_2}{\partial t}=T_w-T_2 \tag{3}$$

where $\overline{T_2}$ denotes the mean air temperature over the row thickness, defined as:

$$\overline{T_2}\left(x^+,t\right)=\int_0^1 T_2\left(x^+,y^+,t\right)dy^+ \tag{4}$$

The symbols $x^+ = x/L_{ch}$ and $y^+ = y/p_2$ in equations (1)–(3) represent dimensionless coordinates. The numbers of heat transfer units N_1 and N_2 are given by:

$$N_1=\frac{h_1 A_{in}}{\dot{m}_1 c_{p1}},\ \ N_2=\frac{h_2 A_{bo}}{\dot{m}_2 c_{p2}} \tag{5}$$

where:

$s = L_{ch}/n_p$
$A_{in} = n_r U_{in} L_{ch},$
$A_{bo} = n_r U_{bo} L_{ch}.$

The time constants τ_1 and τ_2 are:

$$\tau_1 = \frac{m_1 c_{p1}}{h_1 A_{in}} \,, \ \tau_2 = \frac{m_2 c_{p2}}{h_2 A_{bo}} \tag{6}$$

The symbols in equations (1)–(6) denote:

$$m_1 = n_r A_{in} L_{ch} \rho_1, \ m_2 = n_r \left(p_1 p_2 - A_{oval} \right)\left(s - \delta_f \right) n_f \rho_2, \ m_w = n_r U_m \delta_w L_{ch} \rho_w$$

$$m_f = \left(p_1 p_2 - A_{oval} \right) \delta_f \rho_w, \ A_{in} = \pi a b, \ A_{oval} = \pi \left(a + \delta_w \right)\left(b + \delta_w \right), \ U_m = \left(U_{in} + U_{bo} \right)/2.$$

The subscript w refers to the wall, f refers to the fin, and m refers to the mean value.
The weighted heat transfer coefficient h_o is defined by:

$$h_o \left(t \right) = h_2 \left(t \right) \left[\frac{A_{bbf}}{A_{bo}} + \frac{A_f}{A_{bo}} \cdot \eta_f \left(h_2, t \right) \right] \tag{7}$$

The initial temperatures of both fluids are equal and amount to T_0. The initial conditions are:

$$T_1 \left(x^+, t \right)\Big|_{t=0} = T_{1,0} \left(x^+ \right) \tag{8}$$

$$T_w \left(x^+, t \right)\Big|_{t=0} = T_{w,0} \left(x^+ \right) \tag{9}$$

$$T_2 \left(x^+, y^+, t \right)\Big|_{t=0} = T_{2,0} \left(x^+, y^+ \right) \tag{10}$$

The boundary conditions have the following form:

$$T_1 \left(x^+, t \right)\Big|_{x^+=0} = f_1 \left(t \right) \tag{11}$$

$$T_2 \left(x^+, y^+, t \right)\Big|_{y^+=0} = f_2 \left(t \right) \tag{12}$$

$$\frac{\partial T_w}{\partial x}\bigg|_{x=0} = 0 \tag{13}$$

$$\frac{\partial T_w}{\partial x}\bigg|_{x=L_{ch}} = 0 \tag{14}$$

where:

$f_1(t), f_2(t)$ – functions of time describing the variation of the liquid and air temperatures at the inlets to the exchanger.
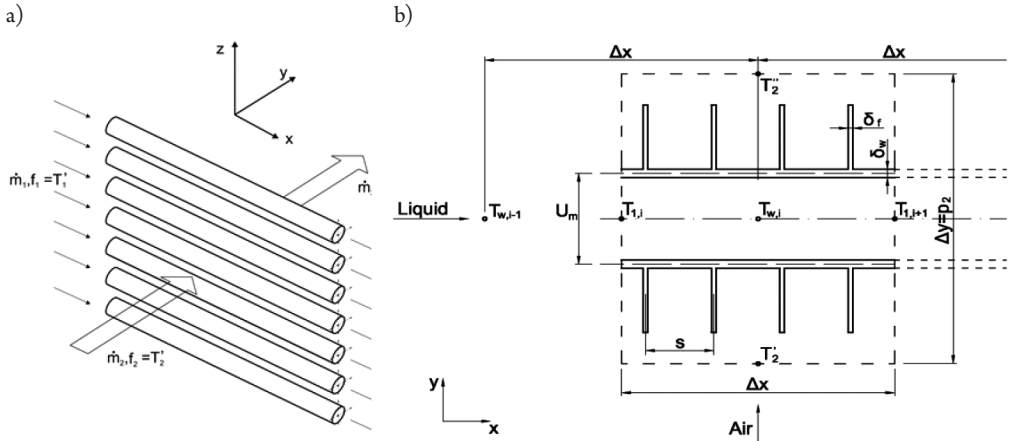
a)   b)

Fig. 1. Scheme of the one-row heat exchanger (a) and control volume (b)

The fin efficiency appearing in a relationship (7) was calculated using the finite volume method based on the finite element method. The division of the fin into finite volumes with specified numbers of nodes is shown in Fig. 2.
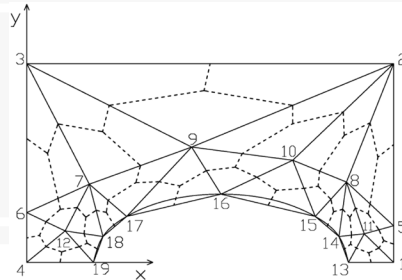

Fig. 2. Division of the fin model into finite volumes with node numbers

The initial-boundary value problem defined by equations (1–14) applies to heat exchangers made of bare or finned tubes. For bare tubes, m_f is equal to zero because there are no fins.

The transient temperatures of the fluids and tube wall in the one-row heat exchanger (Fig. 1) were determined by the explicit finite difference method. To calculate the time-dependent efficiency η_f of the rectangular fin attached to an oval tube, the finite volume – finite element method (FVM-FEM) was used. A mathematical model of the whole heat

exchanger with a complex flow system was built based on the mathematical model of the one-row heat exchanger.

The automotive radiator for a spark-ignition combustion engine with a capacity of 1.580 cm^3 is a double-row, two-pass plate-finned heat exchanger. The radiator consists of aluminium tubes with an oval cross section. The cooling liquid flows in parallel through both tube rows.

3. Experimental correlations for water- and air-side Nusselt numbers

In the developed mathematical model of the exchanger, the heat transfer coefficients on the air and water side are calculated from experimental correlations. The correlations for the heat transfer coefficients are derived assuming a fully developed turbulent flow in straight tubes. One of the most common correlations is the Dittus-Boelter formula [7–9]:

$$\mathrm{Nu}_w = 0.023 \, \mathrm{Re}_w^{0.8} \, \mathrm{Pr}_w^n \left[1 + \left(\frac{d_r}{L_{ch}} \right)^{2/3} \right] \tag{15}$$

where $n = 0.4$ when the fluid is heated and $n = 0.3$ when it is cooled.

Over recent years, the Gnielinski correlation has been becoming more and more popular [10–11].

$$\mathrm{Nu}_w = \frac{(\xi/8)(\mathrm{Re}_w - 1000)\mathrm{Pr}_w}{(1 + 12.7\sqrt{(\xi/8)}(\mathrm{Pr}_w^{2/3} - 1)} \left[1 + \left(\frac{d_r}{L_{ch}} \right)^{2/3} \right] \tag{16}$$

where the friction loss coefficient ξ is defined as:

$$\xi = \frac{1}{(1.82 \log \mathrm{Re}_w - 1.64)^2} = \frac{1}{(0.79 \ln \mathrm{Re}_w - 1.64)^2} \tag{17}$$

In Formula (16), symbols d_r and L_{ch} denote the tube hydraulic diameter and length, respectively. The reason for the growing popularity of the Gnielinski formula (16) is its greater accuracy in the transition area of $2300 < \mathrm{Re}_w < 10000$. Despite the fact that the Gnielinski proposal gives smaller values of the heat transfer coefficient in the transition area compared to the Dittus-Boelter formula, these values are still inflated [12–13]. If $\mathrm{Re}_w < 2300$, the flow is laminar; the Nusselt number is $\mathrm{Nu}_w = 4.364$ and does not depend on the Reynolds number [8–9]. It can be easily checked that both the Dittus-Boelter and the Gnielinski formulae give values of Nu_w much higher than 4.364. For this reason, the correlations for the Nusselt numbers on the water and air side were determined based on experimental testing.

The following form of the correlation for the Nusselt number at the air side was taken:

$$\mathrm{Nu}_a = x_1 \, \mathrm{Re}_a^{x_2} \, \mathrm{Pr}_a^{1/3} \tag{18}$$

Considering that the range of changes in the Reynolds number at the air side is not too wide, it is possible to approximate experimental data effectively using the exponential equation written above (18).

The correlation for the Nusselt number at the water side was taken in a form similar to the formulae developed by Petukhov & Kirillov [14] and Gnielinski [10].

$$\mathrm{Nu}_w = \frac{(\xi/8)(\mathrm{Re}_w - x_3)\mathrm{Pr}_w}{(1 + x_4 \sqrt{(\xi/8)}(\mathrm{Pr}_w^{2/3} - 1))}\left[1 + \left(\frac{d_r}{L_{ch}}\right)^{2/3}\right] \tag{19}$$

The values of coefficients x_1, x_2, …, x_m will be selected so that the sum of the squares of differences in temperature:

$$S = \sum_{i=1}^{n}\left[f''_{w,i} - T''_{w,i}(x_1, ..., x_m)\right]^2 = \min \tag{20}$$

$$f''_{w,i} = T'_{w,i} - \Delta T_{w,i} \tag{21}$$

should reach the minimum.

The real values of the determined parameters $\tilde{x}_1$, …, $\tilde{x}_m$ are included with the probability $P = (1 - \alpha) \cdot 100$ [%] in the following intervals [15–16]:

$$x_i - t_{n-m}^{\alpha/2} \cdot s_t \sqrt{c_{ii}} \le \tilde{x}_i \le x_i + t_{n-m}^{\alpha/2} \cdot s_t \sqrt{c_{ii}} \tag{22}$$

where:

x_i – parameter value determined using the least squares method,

$t_{n-m}^{\alpha/2}$ – t-Student distribution quantile for the confidence level $1 - \alpha$ and $n - m$ degrees of freedom.

Quantity s_t^2 is the variance estimate calculated from:

$$s_t^2 = \frac{\sum_{i=1}^{n}\left[T''_{w,i}(x_1, ..., x_m) - f''_{w,i}\right]^2}{n - m} = \frac{S(\tilde{x}_1, ..., \tilde{x}_m)}{n - m} \tag{23}$$

where:

n – number of measuring points,

m – number of sought parameters.

Quantities c_{ii} are diagonal elements c_{ii} of the covariance matrix.

In this case, the number of measuring points is $n = 47$, and the number of unknown parameters is $m = 4$.

3.1. Measurement results

The thermal and flow measurements of the exchanger were performed for different air and water flow velocities. The measurement results are listed in Table 1.

Table 1. Radiator measurement results

Test run number	$w_{0,i}$ [m/s]	$\dot{V}'_{w,i}$ [l/h]	$T'_{am,i}$ [°C]	$T'_{w,i}$ [°C]	$\Delta T_{w,i}$ [°C]
1	0.40	947. 40	12. 65	62. 21	3. 89
2	0. 66	945. 60	10. 96	62. 24	5. 74
3	0. 92	945. 00	9. 91	62. 14	7. 41
4	1. 18	944. 40	9. 28	62. 04	8. 85
5	1. 44	946. 20	8. 95	61. 95	10. 09
6	1. 70	945. 60	8. 83	61. 70	11. 02
7	1. 96	945. 00	8. 77	61. 35	11. 79
8	2. 22	945. 60	8. 94	61. 14	12. 40
9	2. 22	1150. 80	8. 64	60. 81	10. 87
10	1. 96	1151. 40	8. 65	60. 51	10. 17
11	1. 70	1153. 20	8. 83	60. 24	9. 28
12	1. 44	1152. 60	9. 23	60. 13	8. 48
13	1. 18	1150. 20	8. 96	60. 03	7. 48
14	0. 92	1151. 40	9. 22	60. 04	6. 37
15	0. 66	1150. 80	9. 42	60. 00	5. 13
16	0. 40	1509. 00	11. 56	61. 08	2. 68
17	0. 66	1509. 60	10. 73	61. 10	3. 79
18	0. 92	1510. 20	10. 23	61. 08	4. 85
19	1. 18	1511. 40	9. 87	61. 07	5. 88
20	1. 44	1509. 60	9. 44	60. 94	6. 75
21	1. 70	1508. 40	9. 00	60. 73	7. 57
22	1. 96	1509. 60	8. 98	60. 51	8. 21
23	2. 22	1507. 80	9. 01	60. 30	8. 74
24	2. 22	1842. 60	8. 88	59. 97	7. 42
25	1. 96	1842. 60	8. 90	59. 75	6. 86
26	1. 70	1843. 20	8. 91	59. 47	6. 24
27	1. 44	1840. 20	9. 06	59. 24	5. 54
28	1. 18	1840. 80	9. 13	59. 19	4. 84
29	0. 92	1842. 60	9. 10	59. 17	4. 11
30	0. 66	1840. 20	9. 37	59. 16	3. 25
31	0. 40	1842. 60	9. 88	59. 30	2. 30
32	0. 40	2146. 20	11. 71	60. 02	1. 69
33	0. 66	2146. 20	10. 84	60. 17	2. 54
34	0. 92	2145.60	10. 09	60. 18	3. 39
35	1.18	2143.20	9.52	60.18	4.22
36	1.44	2142.60	9.27	60.07	4.84
37	1.70	2142.60	8.99	59.75	5.46
38	1.96	2139.60	8.96	59.44	5.92
39	2.22	2135.40	9.41	59.22	6.35
40	2.22	2412.00	9.08	58.76	5.70
41	1.96	2413.20	9.12	58.68	5.21
42	1.70	2410.80	9.22	58.40	4.75
43	1.44	2410.80	9.38	58.17	4.23
44	1.18	2410.80	9.10	58.14	3.73
45	0.92	2409.60	9.36	58.23	3.05
46	0.66	2409.60	9.77	58.16	2.46
47	0.40	2410.20	10.05	58.33	1.76

The Reynolds number values at the air side is $\text{Re}_a = w_{max} d_h / v_a$ and at the water side, it is $\text{Re}_{wg} = w_{wg} d_r / v_w$. The physical properties of the air were calculated at the average air temperature. Similarly, the thermophysical properties of water were calculated at the average temperature. The average temperature is understood as the arithmetic mean of the average temperature at the exchanger inlet and outlet. The water velocity in the upper pass w_{wg} is smaller than the water velocity in the lower pass w_{wd} because in the upper pass, water flows in parallel through 20 tubes whereas in the lower one, through 18.

3.2. Experimental correlations

Based on the data presented in Table 1, the following values of individual coefficients were obtained:

$x_1 = 0.0713 \pm 0.0053$; $x_2 = 0.7055 \pm 0.0136$; $x_3 = 0.4624 \pm 0.3194$; $x_4 = 22.2273 \pm 0.3163$

The coefficients are present in Formulae (18) and (19).
The value of the sum of squares is $S = 1.07041 \text{ K}^2$.
The correlations for the Nusselt numbers on the water and air side have the following forms:

$$\text{Nu}_a = 0.0713 \, \text{Re}_a^{0.7055} \, \text{Pr}_a^{1/3}, \; 60 \leq \text{Re}_a \leq 351 \tag{24}$$

$$\text{Nu}_w = \frac{(\xi/8)(\text{Re}_w - 0.4624)\text{Pr}_w}{(1 + 22.2273\sqrt{(\xi/8)}(\text{Pr}_w^{2/3} - 1))} \left[1 + \left(\frac{d_r}{L_{ch}}\right)^{2/3}\right], \; 3850 \leq \text{Re}_w \leq 11317 \tag{25}$$

In the mathematical model of the radiator operation under unsteady-state conditions, relationships (24) and (25) were used.

3.3. The sudden increase in water mass flow rate and the simultaneous reduction in air flow velocity

The comparison of the results obtained from measurements and calculations is presented in Fig. 3.

The water volume flow $\dot{V}_w'$ was increased from about 950 l/h to about 2,400 l/h. Additionally, the air velocity before the exchanger w_0 was reduced from about 2.2 m/s to about 1.2 m/s. Both of these changes contribute to a rise in the water and air temperatures after the exchanger. The smaller velocity of air involves a drop in the heat transfer coefficient on the outer surface of tubes and fins, which in turn decreases the heat flux transferred from water to the flowing air. The air temperature rises after the heat exchanger due to the air mass flow being smaller.
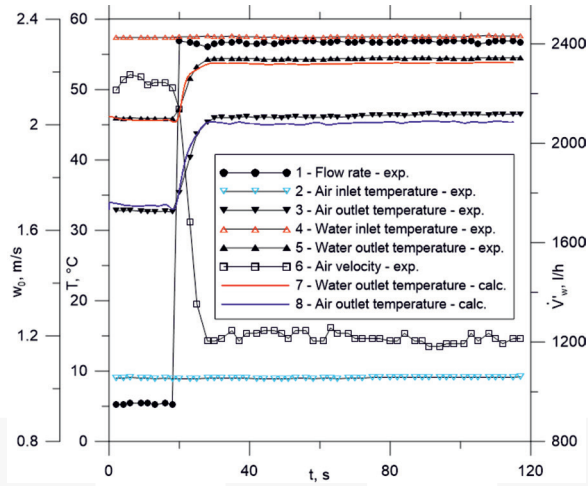
Fig. 3. The exchanger unsteady-state operation caused by a sudden reduction in the water volume flow

1 – $\dot{V}'_w$ – measured water volume flow at the heat exchanger inlet, l/s
2 – T'_{am} – measured mean air temperature at the heat exchanger inlet, °C
3 – T''_{am} – measured mean air temperature after the exchanger, °C
4 – T'_w – measured water temperature at the heat exchanger inlet, °C
5 – T''_w – measured water temperature at the heat exchanger outlet, °C
6 – w_0 – measured air velocity at the heat exchanger inlet, m/s
7 – T''_w – calculated water temperature at the heat exchanger outlet, °C
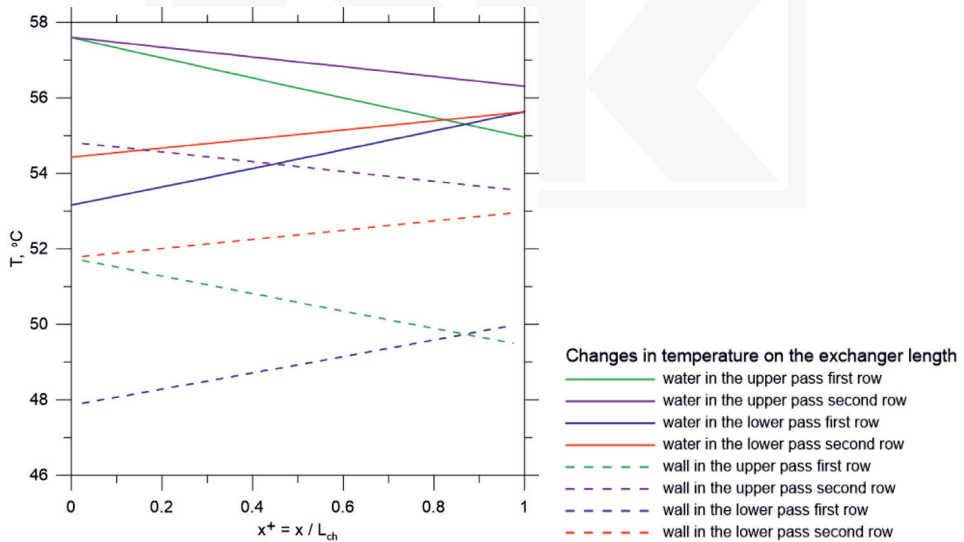8 – T''_{am} – calculated average air temperature at the heat exchanger outlet, °C.

Fig. 4. Distribution of the water and the tube wall temperatures on exchanger length
for time t = 117s in the steady state

Fig. 4 presents changes in the water and the tube wall temperatures on the exchanger length for $t = 117$ s.

In analyzing the results presented in Fig. 4, it can be seen that water in the first row of tubes cools down more than in the tubes placed in the second row. This concerns both the upper and lower pass. It can be observed that the tube wall temperature is lower than the water temperature because cold air absorbs heat.

The curves illustrating time-dependent changes in the temperatures of selected fins are presented in Fig. 5a-d. An analysis of the results indicates that the highest temperature is at the fin base, and the lowest in node 3 (Fig. 2), which is the most distant from the tube axis. It can be seen that the temperatures of the fins in the first tube row (Fig. 5a and 5c) are lower than in the second row (Fig. 5b and 5d). The cold inflowing air cools the fins and tubes located in the first row more effectively. The air temperature after the first tube row is much higher compared to the inlet air temperature. Due to a reduction in the difference between the temperatures of the flowing air and the tubes located in the second row, the temperature of the water and fins in the second tube row is higher than in the first row.
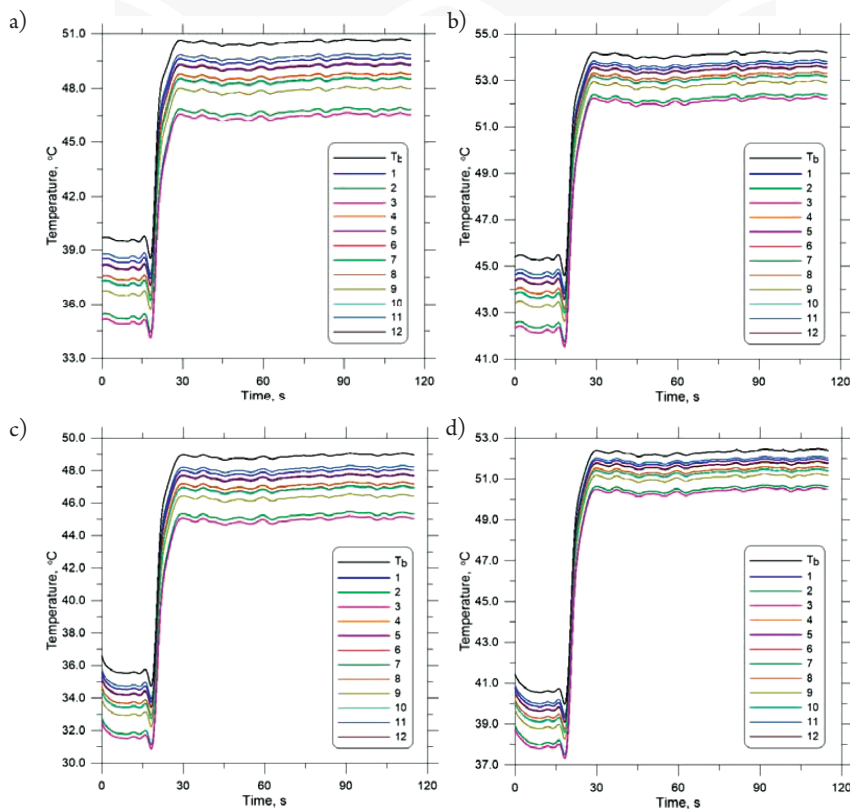

Fig. 5. Changes in the fin base temperature Tb and the fin temperature in 12 nodes that are marked in Fig. 2, at a distance of 247 mm (9.5 cell lengths) from each pass inlet: (a) – first tube row in the first (upper) pass; (b) – second tube row in the first (upper) pass; (c) – first tube row in the second (lower) pass; (d) – second tube row in the second (lower) pass

4. Conclusions

The calculations and measurements carried out in the paper confirm that the developed numerical model of the plate fin and tube heat exchanger has a high level of accuracy. This model is particularly useful to simulate the exchanger, where the temperature of the fins can be very high. Thanks to the experimental determination of heat transfer correlations on the air and water sides, a very strong agreement of calculations and measurements was reached. The developed model can be used to simulate the heating and cooling heat exchanger and in automatic control systems.

References

[1] Taler D., *Mathematical modeling and control of plate fin and tube heat*, Energy Conversion and Management, 96, 2015, 452–462.

[2] Roetzel W., Xuan Y., *Dynamic behaviour of heat exchangers*, Computational Mechanics Publications, Vol. 3, WIT Press, Southampton 1998.

[3] Ataer Ö.E., *An approximate method for transient behavior of finned-tube cross-flow heat exchangers*, Int. J. Refrig., 27, 2004, 529–539.

[4] Taler D., *Direct and inverse heat transfer problems in dynamics of plate fin and tube heat exchangers*, in: Belmiloudi A. (ed.) *Heat transfer, mathematical modelling, numerical methods and information technology*, InTech, Rijeka 2011, 77–100, free online edition: www.intechopen.com.

[5] Vaisi A., Talebi S., Esmaeilpour M., *Transient behavior simulation of fin-and-tube heat exchangers for the variation of the inlet temperatures of both fluids*, International Communications in Heat and Mass Transfer, 38, 2011, 951–957.

[6] Korzeń A., Taler D., *Modeling of transient response of a plate fin and tube heat exchanger*, Int. J. Therm. Sci., 92, 2015, 188–198.

[7] Arpaci V.S., Kao S.H., Selamet A., *Introduction to Heat Transfer*, Prentice Hall, Upper Saddle River, NJ, USA 1999.

[8] Bejan A., Kraus A.D., Ed., *Heat Transfer Handbook*, John Wiley & Sons, Inc., Hoboken, New Jersey 2003.

[9] Wiśniewski S, Wiśniewski T.S., *Wymiana ciepła* (*Heat exchange*), Wydanie 6, WNT, Warszawa 2009.

[10] Gnielinski V., *Neue Gleichungen für den Wärme- und den Stoffübergang in turbulent durchströmten Rohren und Kanälen*, Forschung im Ingenieurwesen, 41/1975 Nr 1, 8–16.

[11] Webb R. L., *Principles of enhanced heat transfer*, John Wiley & Sons, Inc., Hoboken, New Jersey 1994.

[12] Mirth D.R., Ramadhyani S., Hittle D.C., *Thermal performance of chilled-water cooling coils operating at low water velocities*, ASHRAE Transactions, 99, 1993, Part 1, 43–53.

[13] Mirth D. R., Ramadhyani S., *Correlations for predicting the air side Nusselt numbers and friction factors in chilled-water cooling coils*, Experimental Heat Transfer, 7, 1994, 143–162.

[14] Petukhov B.S., Genin A.G., Kovalev S.A., *Heat transfer in nuclear power plants*, Atomizdat, Moscow 1974 (in Russian).

[15] Brandt S., *Data Analysis. Statistical and computational methods for scientists and engineers*, 3rd edn. Springer, Berlin 1999.

[16] Coleman H.W., Steele W.G., *Experimentation, validation, and uncertainty analysis for engineers*, 3rd edn. Wiley, Hoboken 2009.